RSC Advances

ROYAL SOCIETY OF CHEMISTRY

www.rsc.org/advances

ChemComm

RSCPublishing

COMMUNICATION

Robust and antireflective superhydrophobic surfaces prepared by CVD of cured polydimethylsiloxane with candle soot as a template

Cite this: DOI: 10.1039/x0xx00000x

Received 00th January 2014,
Accepted 00th January 2014

DOI: 10.1039/x0xx00000x

www.rsc.org/

Xiaojiang Liu [a], Yang Xu [a], Zao Chen [a], Keyang Ben [a], and Zisheng Guan* [a]

Taking candle soot as a template, cured polydimethylsiloxane (PDMS) is firstly used for CVD at a high temperature in air to create robust and antireflective superhydrophobic surfaces. No organic solutions or chemical modification is needed. Three-phase lines of the surface are studied by observing the light projection view.

Because of the excellent characteristics including water-repellency, self-cleaning, anti-icing and drag-reduction, superhydrophobic surfaces have gained much attention in the past decades.[1-6] To obtain these surfaces, hierarchical or micro/nano structures are essential, and except a few examples,[7] almost all superhydrophobic surfaces are made from or on low surface energy materials. In some practical areas such as windshields, lenses and glass of solar cells, besides self-cleaning, transparency is a must and antireflection is a better choice.[8-12] Meanwhile, if these surfaces combine robust properties,[13] for example, resistance to impact of water and dust particles, repellency to acid and basic solution and thermal stability, they will find a wider application.

Plasma etching,[14, 15] soft lithography,[16, 17] sol–gel,[18, 19] phase separation,[20, 21] templating method,[22] and nanoparticle assembly[23, 24] are now general methods adopted to prepare transparent superhydrophobic surfaces. Among these approaches, templating method is a good approach that usually involves four steps: fabrication of a template, creation of structures on the template, calcination to remove the template and hydrophobilization. This method can construct porous stuctures that are helpful to improve the superhydrophobicity and transparency. Recently, carbon nanometer materials have become a hot topic in the preparation of superhydrophobic surfaces due to their desirable structures.[25-29] They are also used as templates to prepare transparent superhydrophobic surfaces[30-32] because a thermal oxidation process is able to remove them. In a templating method, chemical vapor deposition (CVD) methods were widely used for either creation of structures, or modification of low surface energy substances, *e.g.* hydrolysis and condensation of tetraethylorthosilicate and modification of semi-fluorinated silane.[30, 32] But, because the raw materials were usually liquid and extremely reactive, these CVD often demanded sophisticated equipment and harsh conditions and could not obtain rough structures and low surface energy within one step. Besides, in almost every reported template method, the common-used four steps were all involved and the costly semi-fluorinated silane was often employed to reduce the surface energy. So, it would be a significant progress to achieve antireflective superhydrophobic surfaces with low cost and fewer operations.

Herein, taking candle soot as a template, we firstly use cured PDMS for CVD to create antireflective superhydrophobic surfaces by controlling the amount of cured PDMS, the temperature and the holding time. It is notable that this novel CVD is carried out in air at a high temperature and no special instruments or atmosphere is necessary. The usually used four steps have been simplified into two steps: (1) deposition of candle soot and (2) CVD of PDMS and oxidization of the candle soot within one-step heat process. A series of tests have confirmed that these surfaces have excellent ability of resistance to impact of water and dust particles, repellency to acid and basic solution.

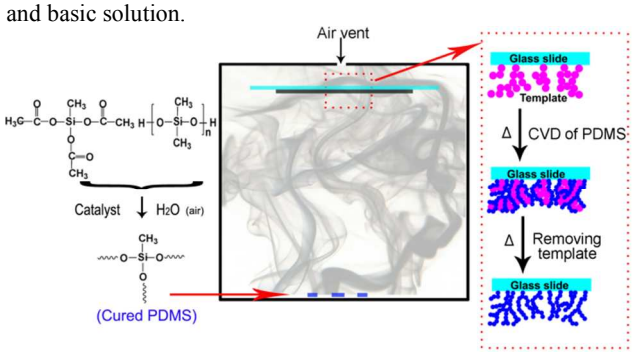

Fig. 1 Schematic illustration for preparing the superhydrophobic surfaces.

Fig. 1 demonstrates the formation process of the superhydrophobic surfaces. The cured PDMS is prepared by mixing triacetoxy(methyl)silane, α, ω- dihydroxypolydimethylsiloxane and

dibutyltin dilaurate (DBTDL) in air, in which DBTDL is adopted as a catalyst to accelerate the curing reaction. The PDMS can decompose at a high temperature in air that the major degradation products are a mixture of oligomers including cyclic organic oligomers.[33] Meanwhile, these organic oligomers are not so stable in air at a high temperature that a CVD reaction will occur to them with the help of oxygen in air, contributing to the CVD product. The pores of the deposited candle soot give space for the CVD product to penetrate in and attach to the candle soot and to each other. As heating proceeds, the candle soot can be removed through an oxidization process at a higher temperature and the nano-sized and porous structures are finally created. The processes of CVD of PDMS and removing template can be finished within one-step heat treatment to reduce multiple operations. The TG curves (Fig. S1, ESI†) and the FT-IR spectra (Fig. S2, ESI†) show that the CVD product can keep its surface energy low until about 535 °C, indicating its higher thermal stability than the candle soot that can be oxidized when the temperature is higher than 400 °C. So, it is necessary to control the temperature within the range of 400-535 °C to prepare superhydrophobic surfaces. In our experiments, the temperature is controlled at 405 °C and the holding time is controlled at 80 min. Here, using inexpensive PDMS as raw materials for CVD can be a good candidate for the existing traditional CVD and can obtain porous structures with low surface energy that are essential for superhydrophobicity.

Table 1 The dependence of water contact angle (WCA), sliding angle (SA) and average transmittance (AT) (400-800 nm) on the amount of the cured PDMS

PDMS/mg	Bare glass	3.6	4.8	5.9	7.2	8.0	9.2
WCA/°	5.5	155	157	156	157	157.5	158
SA/°	—	4	3.5	3.5	3	3	2
AT/%	90.12	89.36	88.15	90.83	91.32	87.85	84.09

Also because of the nano-sized and porous structures, these superhydrophobic surfaces are highly transparent.[34] Table 1 lists the values of WCA, SA and average transmittance of the superhydrophobic surfaces prepared with different amount of cured PDMS. It is shown that the superhydrophobicity was not obviously changed by the amount of the cured PDMS used in the CVD reaction. The surfaces with 7.2 mg PDMS have a WCA of 157° and a SA of 3°, as well as a ~1.2% higher average transmittance than the bare glass slides in the visible range (400-800 nm). This result is very ideal compared to the other reported similar templating methods.[13, 30-32] Fig. 2a and 2c show the photographs of candle soot coated glass and antireflective superhydrophobic glass prepared by CVD of PDMS, on which water droplets and ink droplets deposited. Compared to candle soot (Fig. 2b) that has a diameter of ~60 nm, the CVD particles prepared with 7.2 mg cured PDMS have a smaller size of ~30 nm (Fig. 2d) and the thickness decrease from ~ 20 μm to less than 300 nm (Fig. S3, ESI†), which is smaller than the wavelength of the visible light. Besides, the CVD particles can attach to each other to form fibrous and porous structures (Fig 2e). The size of the nanometer scale structures is much smaller than the wavelength of the visible light, which can effectively reduce the refractive index of the bare glass substrates and increase the transmittance. If more cured PDMS is used, the size of the CVD particles become larger and the porous structures are restricted (Fig 2f), leading to a loss of light transmittance. So, by controlling the amount of cured PDMS, it is very facile to obtain superhydrophobicity with high transmittance or even antireflection.

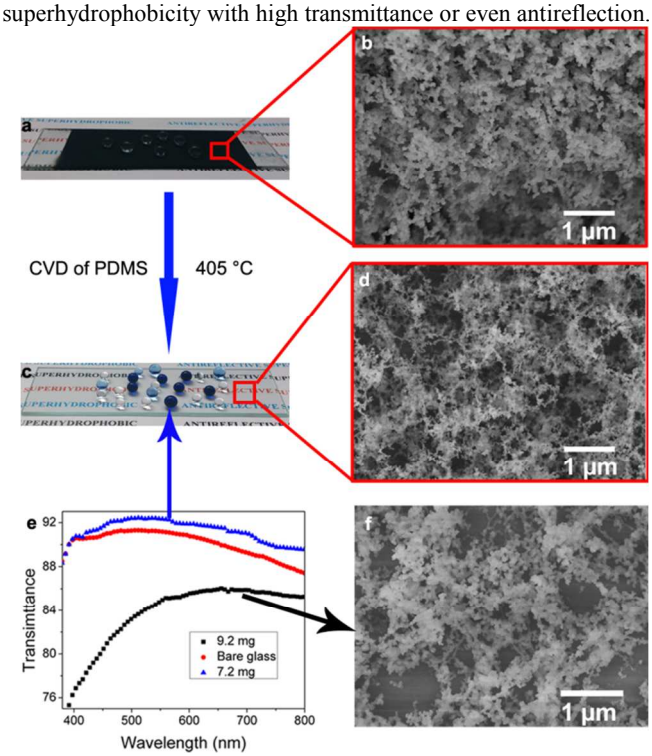

Fig. 2 (a, c) photographs of the candle soot coated glass and antireflective superhydrophobic glass prepared by CVD of 7.2 mg cured PDMS, on which water droplets and ink droplets deposited. (b, d, f) SEM images of the candle soot, the superhydrophobic surfaces prepared by CVD of 7.2 and 9.2 mg cured PDMS. (e) Transmittance of the bare glass and the the superhydrophobic glass prepared by CVD of 7.2 and 9.2 mg cured PDMS.

For the bare glass slides without coated candle soot, after CVD treatment they are also hydrophobic but far from superhydrophobic, which is due to the absence of template that results in poor roughness (Fig. S4, ESI†). On the other hand, although the candle soot coated surfaces show superhydrophobicity with a WCA of 156 ± 1° and a SA less than 3°, they suffer from low transmittance and can be destroyed easily by the depositing of water droplets (Fig. S5, ESI†) due to the van der Waals interactions between soot particles.13 However, the candle soot coated surfaces after CVD of PDMS at 370 °C could keep the superhydrophobicity even after the soot is removed by water flow impact (Movie S1, ESI†), meaning the adhesive force of the surfaces was enhanced and chemical bonds have been formed between the CVD particles and between the slides and the CVD particles. At this stage, part of unoxidized candle soot existed accompanied by the CVD particles (Figure S6, ESI†). At a higher temperature, for example, 405 °C, the candle soot is completely removed and the enhanced adhesive force is kept.

Besides the thermal stability mentioned in the TG curves above, a series of tests were carried out to confirm their robustness,

including repellency to acid and basic solution, resistance to impact of water and dust particles. First, these surfaces exhibit superhydrophobicity for aqueous solutions of different pH values (Fig. S7, ESI†). Second, similar to early report,[30] we set a 10 cm height and controlled a bigger droplet size of 12 µL to study the ability of water droplet-impact resistance. The water droplets were bounced off upon contacting the surfaces, as shown in Fig. 3a and the supporting information (Movie S2, ESI†). The antireflective superhydrophobic surfaces prepared with 7.2 mg PDMS did not show hints of altering until impinging of 330 800 water droplets. Meanwhile, the antireflection did not show obvious decrease after impinging of 250 000 water droplets and the average transmittance in the visible range only decreases from ~91.32 to ~91.30. If more PDMS was used, the number is increased, e.g. 830 700 for 9.2 mg PDMS, but at the cost of the loss of the transmittance. In a third test, the antireflective superhydrophobic slides were pushed and pulled at a speed of 4 cm/s in water to test the stability of the whole surfaces. The title angle is 45° and the moving distance is 7 cm (Fig. S8, ESI†). The surface did not lose the superhydrophobicity until the number of cycles was up to 620. The latter two tests implied that the superhydrophobic surfaces obtained within two steps in our experiments are strongly attached to the glass substrates.

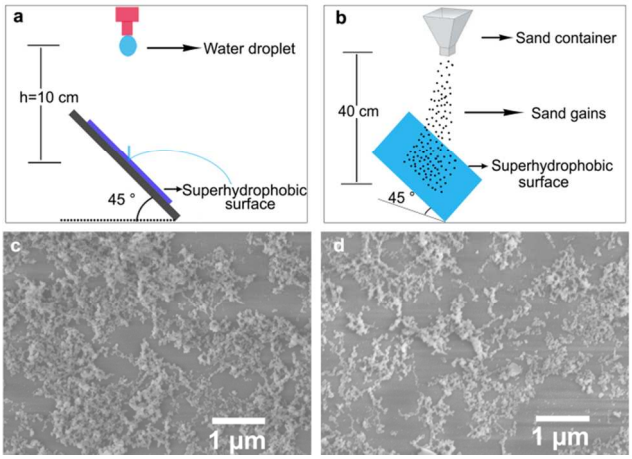

Fig. 3 Schematic illustrations of water (a) and sands (b) impact on the superhydrophobic surfaces, respectively. SEM images of the surfaces that still keep superhydrophobic (c) and begin to loss superhydrophobicity (d) after sands impact.

When used in daily life, these superhydrophobic surfaces are subjected to the impact of dust particles. Here, sand gains are impacted on an antireflective superhydrophobic surface at a height (h) of 40 cm to simulate this situation. The diameters of the sand gains (Rs) are 100 to 200 µm and 200 to 400 µm and the flow rate is 10 g/min. It is calculated that the impact velocity ($v_s = (2\ g\ h)^{1/2}$) is 2.8 m/s and the impact energy ($Ws = m_s\ g\ h = 4/3\ \pi\ \rho\ R_s^3\ g\ h$) is 4.35 × 10^{-8} J (R_s = 100 µm) and 3.48 × 10^{-7} J (R_s = 200 µm). Here, ρ is the density of silica ($\rho \approx 2.65$ g/cm3) and g is the acceleration of gravity ($g \approx 9.8$ m/s^2). Results indicated that in order to make the surfaces lose the superhydrophobiciy, the mass of the sand gains used were 18 g (R_s = 100 to 200 µm) and 10 g (R_s = 200 to 400 µm). These numbers also confirmed the high robustness of the superhydrophobic surfaces. Figure 3c and 3d show the SEM images of the surface that still keeps superhydrophobic and the surface begins to lose superhydrophobicity. These images indicate that the impact of sand gains damaged the superhydrophobic surfaces by gradually breaking the structures and removing the particles.

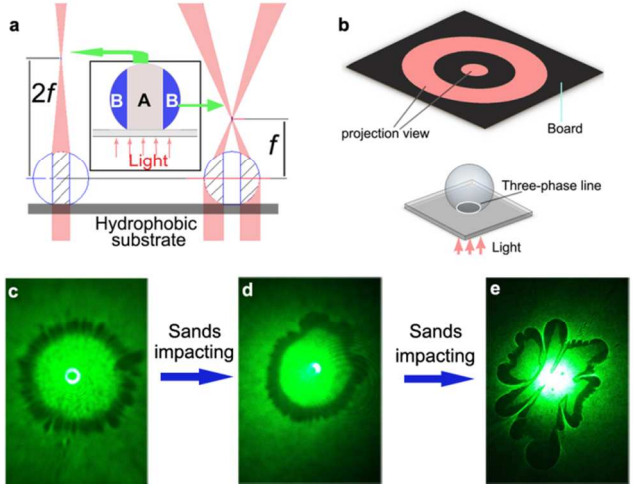

Fig. 4 (a) Schematic illustration of a parallel light irradiating a water droplet on a highly hydrophobic surface. The droplet can be seen as two parts: part A and part B, whose vertical projection are inside and outside the three-phase line, respectively. (b) A 3D view of a water droplet on a highly hydrophobic surface (down) and schematic illustration of the projection view of a parallel light irradiating the water droplet on the surface (top). Photographs of the green light projection view of an 8 µL water droplet on a superhydrophobic surface (c) and the superhydrophobic surfaces after sands impact (d, e). The extent of the damage ranges from low to high and the surfaces all keep hydrophobic after impact.

When studying the optical behaviors of water droplets on a transparent and highly hydrophobic surface, we assume that a water droplet is part of a sphere that has a platform, and then a droplet can be regarded as two parts when light irradiate the droplet in parallel (see the insert in Fig. 4a). The focal lengths are 2 f (left in Fig. 4a) and f (right in Fig. 4a) by calculating focal length: F = $n\ R/(n\text{-}1)$ and f = $n\ R/2\ (n\text{-}1)$, where n is the refractive index for water and R is the radius of water. When a board is put horizontally at a distance > 2f above the water droplet, a projection view like the top figure in Fig. 4b will be observed. The sideline of the dark ring corresponds to the projection of the three-phase line of the droplet. This method is especially useful to those with superhydrophobicity whose three-phase lines are not easy to distinguish by other methods. Figure 4c shows the photograph of the projection of a water droplet on the superhydrophobic surfaces prepared with 9.2 mg cured polysiloxnaes. The sideline of the dark ring in the projection was an unenclosed circle with lots of petals, meaning the water droplet on our superhydrophobic surface has a discontinuous three-phase line. This discontinuous three-phase line forms due to lots of unclosed pockets under the droplet, which contributes to a small SA.[35, 36] If the superhydrophobic surface was damaged, for example by sands impact, the sideline would be enclosed and out of shape. And a larger deformation of the triple-phase line usually corresponds to a larger damage or more serious uniformity for the surface (see Fig. 4d-e). So, the light projection view could be a simple way to detect

the condition of a highly hydrophobic surface with transparency or semi-transparency.

In conclusion, robust and antireflective superhydrophobic surfaces have been successfully and facilely created with candle soot as a template. Cured PDMS used for CVD in air makes the operation more facile and gets rid of expensive instruments and materials as well as harsh operation condition. Though a CVD process at a high temperature, the candle soot template is oxidized and porous structures is easily obtained without damaging the low surface energy. The excellent robustness and antireflection can expand the superhydrophobic surfaces great potential in many practical uses. We also study the three-phase lines and detect the condition of highly hydrophobic surfaces by observing the light projection view.

This work was supported by the National Natural Science Foundation of China (20573055, 21071081) and a project funded by the Priority Academic Program Development of Jiangsu Higher Education Institutions of China. We greatly thank State Key Laboratory of Materials-Oriented Chemical Engineering for help during experiments.

Notes and references

[a] *College of Materials Science and Engineering, Nanjing Tech University, Nanjing, 210009, P. R. China. E-mail: zsguan@njtech.edu.cn*

† Electronic supplementary information (ESI) available: Experimental details and supplementary materials. See DOI: 10.1039/c000000x/

1 Q. D. Xie, J. Xu, L. Feng, L. Jiang, W. H. Tang, X. D. Luo and C. C. Han, *Adv. Mater.*, 2004, **16**, 302-305.
2 A. Tuteja, W. Choi, M. Ma, J. M. Mabry, S. A. Mazzella, G. C. Rutledge, G. H. McKinley and R. E. Cohen, *Science*, 2007, **318**, 1618-1622.
3 X. Yao, Y. L. Song and L. Jiang, *Adv. Mater.*, 2011, **23**, 719-34.
4 Y. L. Zhang, H. Xia, E. Kim and H. B. Sun, *Soft Matter*, 2012, **8**, 11217–11231.
5 Z. L. Chu and S. Seeger, *Chem. Soc. Rev.*, 2014, **43**, 2784-2798.
6 H. Zhu, Z. G. Guo and W. M. Liu, *Chem. Commun.*, 2014, **50**, 3900-3913.
7 L. Cao, H. H. Hu and D. Gao, *Langmuir*, 2007, **23**, 4310-4314.
8 Y. Li, F. Liu and J. Sun, *Chem. Commun.*, 2009, 2730-2732.
9 G. R. J. Artus, S. Jung, J. Zimmermann, H. P. Gautschi, K. Marquardt and S. Seeger, *Adv. Mater.*, 2006, **18**, 2758-2762.
10 S. Kim, J. Cho and K. Char, *Langmuir*, 2007, **23**, 6737-6743.
11 Y. Rahmawan, L. Xu and S. Yang, *J. Mater. Chem. A*, 2013, **1**, 2955–2969.
12 G. Zhou, J. H. He, L. J. Gao, T. T. Ren and T. Li, *RSC Adv.*, 2013, **3**, 21789–21796.
13 X. Deng, L. Mammen, Y. Zhao, P. Lellig, K. Mullen, C. Li, H. J. Butt and D. Vollmer, *Adv. Mater.*, 2011, **23**, 2962-2965.
14 A. Irzh, L. Ghindes and A. Gedanken, *ACS Appl. Mater. Interfaces*, 2011, **3**, 4566-4572.
15 S. H. Hsu, Y. L. Chang, Y. C. Tu, C. M. Tsai and W. F. Su, *ACS Appl. Mater. Interfaces*, 2013, **5**, 2991-2998.
16 S. H. Lee, K. S. Han, J. H. Shin, S. Y. Hwang and H. Lee, *Prog. Photovoltaics*, 2013, **21**, 1056-1062.
17 J. H. Kong, T. H. Kim, J. H. Kim, J. K. Park, D. W. Lee, S. H. Kim and J. M. Kim, *Nanoscale*, 2014, **6**, 1453-1461.
18 X. Y. Li, X. Du and J. H. He, *Langmuir*, 2010, **26**, 13528-13534.
19 J. B. Lin, H. L. Chen, T. Fei, C. Liu and J. L. Zhang, *Appl. Surf. Sci.*, 2013, **273**, 776-786.
20 S. Kato and A. Sato, *J. Mater. Chem.*, 2012, **22**, 8613-8621.
21 Z. F. Wu, H. Wang, X. Y. Tian, P. Cui, X. Ding and X. Z. Ye, *Phys. Chem. Chem. Phys.*, 2014, **16**, 6787-6794.
22 B. G. Park, W. Lee, J. S. Kim and K. B. Lee, *Colloids Surf., A*, 2010, **370**, 15-19.
23 L. B. Xu, R. G. Karunakaran, J. Guo and S. Yang, *ACS Appl. Mater. Interfaces*, 2012, **4**, 1118-1125.
24 U. Manna, A. H. Broderick and D. M. Lynn, *Adv. Mater.*, 2012, **24**, 4291-4295.
25 M. N. Qu, J. M. He and B. Y. Cao, *Appl. Surf. Sci.*, 2010, **257**, 6-9.
26 C. J. Liang, J. D. Liao, A. J. Li, C. Chen, H. Y. Lin, X. J. Wang and Y. H. Xu, *Fuel*, 2014, **128**, 422-427.
27 K. Seo, M. Kim and D. H. Kim, *Carbon*, 2014, **68**, 583-596.
28 F. Zhao, L. L. Liu, F. J. Ma and L. Liu, *RSC Adv.*, 2014, **4**, 7132–7135.
29 A. Asthana, T. Maitra, R. Buchel, M. K. Tiwari and D. Poulikakos, *ACS Appl. Mater. Interfaces*, 2014, **6**, 8859-8867.
30 X. Deng, L. Mammen, H. J. Butt and D. Vollmer, *Science*, 2012, **335**, 67–70.
31 S. H. Liu, M. Sakai, B. S. Liu, C. Terashima, K. Nakata and A. Fujishima, *RSC Adv.*, 2013, **3**, 22825–22829.
32 X. T. Zhu, Z. Z. Zhang, G. Ren, X. H. Men, B. Ge and X. Y. Zhou, *J. Colloid Interface Sci.*, 2014, **421**, 141-145.
33 G. Camino, S. M. Lomakin and M. Lazzari, *Polymer*, 2001, **42**, 2395-2402.
34 R. G. Karunakaran, C. H. Lu, Z. Zhang and S. Yang, *Langmuir*, 2011, **27**, 4594-602.
35 Y. K. Lai, X. F. Gao, H. F. Zhuang, J. Y. Huang, C. J. Lin and L. Jiang, *Adv. Mater.*, 2009, **21**, 3799-3803.
36 S. G. Lee, D. S. Ham, D. Y. Lee, H. Bong and K. Cho, *Langmuir*, 2013, **29**, 15051-15057.

